

## Experimental evidence for 400-meV valence-band dispersion in solid C<sub>60</sub>

G. Gensterblum, J.-J. Pireaux, P. A. Thiry, and R. Caudano

*Laboratoire Interdisciplinaire de Spectroscopie Electronique, Facultés Universitaires Notre-Dame de la Paix, 61, rue de Bruzelles, B-5000 Namur, Belgium*

T. Buslaps and R. L. Johnson

*II. Institut für Experimentalphysik, Universität Hamburg, Luruper Chaussee 149, D-22761 Hamburg, Germany*

G. Le Lay and V. Aristov

*Centre de Recherche sur les Mécanismes de la Croissance Cristalline, Campus de Luminy, Case 913, F-13288 Marseille Cedex 9, France*

R. Günther, A. Taleb-Ibrahimi, G. Indlekofer, and Y. Petroff

*Laboratoire pour l'Utilisation du Rayonnement Electromagnétique, Centre Universitaire de Paris-Sud, Bâtiment 209d, F-91405 Orsay, France*

(Received 24 August 1993)

Angle-resolved electron distribution curves have been measured for two different excitation energies on heteroepitaxial C<sub>60</sub>(111) films. At  $\hbar\omega = 29$  eV, the limited  $k_{\parallel}$  resolution together with broadening induced by vibronic excitations results in a weak dependence of the peak positions and line shapes of the photoemission features on the emission angle. We demonstrate that at the low photon energy of  $\hbar\omega = 8.1$  eV the  $k_{\parallel}$  resolution becomes sufficient to resolve two bands in the feature derived from the highest-occupied molecular orbital which show a dispersion of the order of 400 meV.

C<sub>60</sub> fullerite is a molecular solid,<sup>1</sup> whose electronic properties are essentially determined by the covalent bonding within individual molecules. The valence- and conduction-band spectra of solid C<sub>60</sub> as measured by direct<sup>2</sup> and inverse photoemission<sup>3</sup> exhibit very sharp spectral features which compare well with the electronic states obtained from molecular cluster calculations.<sup>4</sup> Furthermore, the photoemission spectra recorded from the solid and gas phases are quite similar.<sup>5</sup> Hence, the electronic energy levels of the C<sub>60</sub> molecules are only slightly perturbed by band formation due to electron interactions between the C<sub>60</sub> molecules in the solid state. Nevertheless, a detailed knowledge of the band structure and especially the bandwidth are important issues for understanding many properties of the fullerenes.

From a theoretical point of view the band structure has been extensively studied and calculations predict an energy dispersion of 400–500 meV.<sup>1,6</sup> On the experimental side, Wu *et al.*<sup>7</sup> reported angle-resolved photoemission measurements at  $\hbar\omega = 25$  eV on a small C<sub>60</sub> single crystal (0.3×0.4 mm<sup>2</sup>). They observed no significant energy dispersion [the highest occupied molecular orbital (HOMO) derived band disperses as little as 50 meV] and only small changes in the photoemission line shape and peak width over a wide range of crystal momentum (**k**). Furthermore, since the gas-phase photoemission spectrum<sup>5</sup> of the HOMO state is also very broad, and can be resolved into at least two features, they conclude that the dispersion of individual bands is small and the width of the valence band in photoemission is broadened by transitions to excited vibrational states and does not reflect the intrinsic bandwidth.

In this paper, we present angle-resolved electron distribution curves (EDC's) on heteroepitaxial C<sub>60</sub>(111) films grown on GeS(001).<sup>8,9</sup> The use of such films for photoemission measurements has several advantages over C<sub>60</sub> single crystals. In particular the small size of available single crystals may give rise to a high background and a limited count rate. Furthermore, insulating C<sub>60</sub> crystals exhibit charging effects which have to be compensated.<sup>7</sup>

The heteroepitaxial C<sub>60</sub>(111) films were grown *in situ* on a GeS(001) single crystal (7×7 mm<sup>2</sup>).<sup>8,9</sup> The film was about 120 Å thick which was enough to attenuate the substrate emission completely. The angle-resolved EDC's have been recorded on the high resolution SU3 beamline at the Laboratoire pour l'Utilisation du Rayonnement Electromagnétique (LURE, Paris) with a photon energy of  $\hbar\omega = 29$  eV and at lower photon energies on the Seya-Namioka beamline at the Hamburg Synchrotron Radiation Laboratory (HASYLAB). The overall energy resolution was about 100 meV for both experiments.

Figure 1 shows raw data of the first two valence-band peaks in the form of EDC's recorded at different emission angles ( $\theta_e$ ) along the  $\bar{\Gamma}$ - $\bar{K}$ - $\bar{M}$  direction of the surface Brillouin zone (SBZ) with a photon energy of 29 eV. The energies are measured with respect to the Fermi level of a clean rhodium plate, which is part of the manipulator. The  $\bar{\Gamma}$ ,  $\bar{K}$ , and  $\bar{M}$  points correspond, respectively, to normal, 10°, and 15° emission angles. Although the width of the photoemission peaks is much larger than our resolution, the individual bands (e.g., the HOMO-derived feature at -2.6 eV is fivefold degenerate) are not resolved. The maximum of the asymmetric HOMO peak shows only limited dispersion and no significant change

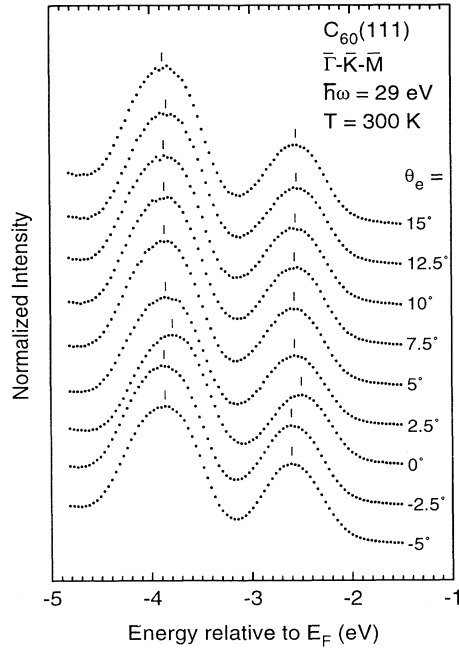


FIG. 1. Set of EDC's of the first two valence bands of  $C_{60}$  for different emission angles ( $\theta_e$ ) recorded in the  $\bar{\Gamma}$ - $\bar{K}$ - $\bar{M}$  direction with a photon energy of  $\hbar\omega = 29$  eV.

of the line shape with emission angle is observed. One could argue that the shift of about 100 meV observed at the zone center, i.e., for normal emission, may be an experimental artifact. We shall show later that this apparent maximum at  $\bar{\Gamma}$  is physically relevant.

As pointed out by Wu *et al.*<sup>7</sup> the small observed dispersion can be explained by a broadening caused by transitions to excited vibrational states. On the other hand, since  $C_{60}$  fullerite has a large lattice parameter [ $a = 14.17$  Å at 300 K (Ref. 10)] its Brillouin zone is very small. The dimensions of the SBZ in the  $\bar{\Gamma}$ - $\bar{K}$  and  $\bar{\Gamma}$ - $\bar{M}$  directions are  $k_{\parallel}^{\bar{\Gamma}\bar{K}} = 4\pi\sqrt{2}/3a = 0.418$  Å<sup>-1</sup> and  $k_{\parallel}^{\bar{\Gamma}\bar{M}} = 2\pi\sqrt{2}/\sqrt{3}a = 0.362$  Å<sup>-1</sup>. At a photon energy of 29 eV, the wave-vector component parallel to the surface, associated with the maximum of the HOMO-derived feature is given by  $k_{\parallel} = 2.37 \sin \theta_e$  (Å<sup>-1</sup>). Consequently the zone boundary is reached for an emission angle of about 10° (9°) in the  $\bar{\Gamma}$ - $\bar{K}$  ( $\bar{\Gamma}$ - $\bar{M}$ ) direction. With a typical analyzer acceptance  $\Delta\theta_a \sim 2^\circ$  this implies that each spectrum in Fig. 1 integrates over about 20% of the SBZ. It is then plausible that averaging over such a sizable part of the SBZ together with broadening induced by vibronic excitations wipes out the individual bands and produces one single broad asymmetric peak whose centroid and shape hardly vary as a function of the particular wave vector of the SBZ around which one is integrating, especially since the intrinsic band dispersion is small.

In order to resolve the individual bands in the SBZ, one has to decrease drastically the photon energy so as to improve the  $k_{\parallel}$  resolution. Figure 2 shows a set of EDC's (raw data) of the HOMO-derived feature recorded in the  $\bar{\Gamma}$ - $\bar{K}$  azimuth with a photon energy of  $\hbar\omega = 8.1$  eV. The energies are referenced to the Fermi level of a tan-

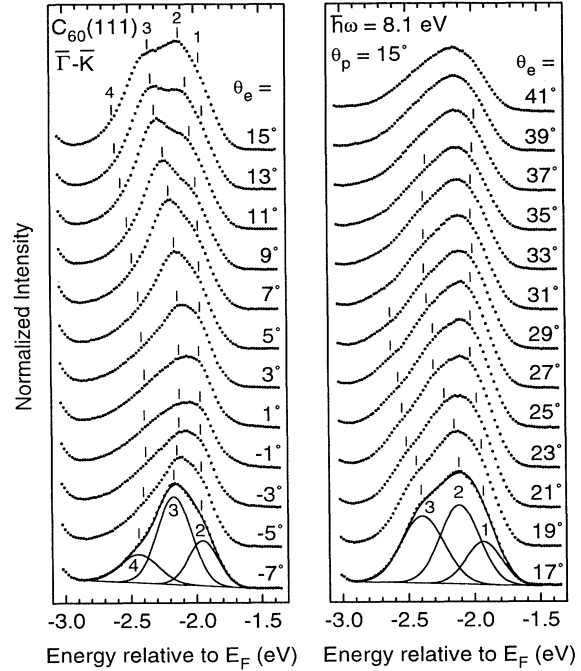


FIG. 2. Set of EDC's of the HOMO-derived feature for different emission angles ( $\theta_e$ ) recorded in the  $\bar{\Gamma}$ - $\bar{K}$  direction with a photon energy of  $\hbar\omega = 8.1$  eV. Representative results of the fit procedure are shown for  $\theta_e = 7^\circ$  and  $17^\circ$ . The tick marks indicate the positions of the maxima of the four peaks obtained from the fit.

talum foil. At this low photon energy the cutoff of the analyzer occurs in the second peak and from its position the work function of  $C_{60}$  can be determined to be  $e\phi = 4.7$  eV. The wave vector parallel to the surface associated with the maximum located at  $E_i = -2.2$  eV is given by  $k_{\parallel} = 0.51\sqrt{\hbar\omega - e\phi + E_i} \sin \theta_e = 0.56 \sin \theta_e$  (Å<sup>-1</sup>), so the zone boundary is reached at an emission angle of about 48° (40°) in the  $\bar{\Gamma}$ - $\bar{K}$  ( $\bar{\Gamma}$ - $\bar{M}$ ) direction. The  $k_{\parallel}$  resolution,  $\Delta k_{\parallel} = 0.56 \cos \theta_e \Delta \theta_a$ , varies from 0.020 Å<sup>-1</sup> to 0.013 Å<sup>-1</sup> for normal and 48° emission angles, respectively. This corresponds to between 4.8% and 3.1% of the dimension of the SBZ when moving from the zone center to the zone boundary along the  $\bar{\Gamma}$ - $\bar{K}$  direction, which is reasonable for angle-resolved measurements.

In Fig. 2 significant changes of the line shape with emission angle can be seen; two components are clearly resolved at some emission angles (13° and 15°), and their dispersion can be followed up to emission angles of 21°. The maximum of the photoemission feature at low angles (peak 3) shows a dispersion of the order of 400 meV and shrinks into a shoulder for higher emission angles. On the other hand, the pronounced shoulder (peak 2) observed at low angles (e.g., at 7°) which develops into a well-resolved peak with increasing emission angle and becomes the dominant feature for high emission angles, shows a smaller dispersion. The data recorded in the  $\bar{\Gamma}$ - $\bar{M}$  direction (not shown here) are very similar around the zone center, but are somewhat different in the second half of the SBZ as far as the peak intensity is concerned. Al-

though there are only two components which are clearly visible in both directions, the line shapes of the different photoemission peaks suggest that it consists of at least four components. We found that the HOMO-derived feature could not be fitted well with less than four bands. In order to retrieve the energy position of the individual bands we have used a maximum likelihood fit algorithm<sup>11</sup> assuming Gaussian line shapes for the individual bands. The quality of the fitting procedure can be judged from the two representative results shown in Fig. 2 for emission angles of  $-7^\circ$  and  $17^\circ$ .

Figure 3 shows the energy dispersion curves along the  $\bar{\Gamma}$ - $\bar{K}$  azimuth obtained from the peak positions produced by the fit. We estimate the uncertainty in the peak position to be about 100 meV. The two upper bands (peaks 1 and 2) seem to originate from the same degenerated energy level at  $\bar{\Gamma}$  which splits when moving away from the zone center. While the upper band only shows small dispersion, the lower one disperses by as much as 400 meV with a broad maximum around  $\bar{\Gamma}$ . In all of the fits, the two lower bands (peaks 3 and 4) always appeared at the same energy position with respect to the second band; the energy separations are about 200 meV to band 3 and 400 meV to band 4. It is clear that a detailed knowledge of the band structure can only be obtained by comparing our photoemission spectra with sophisticated theoretical calculations which take into account electron-phonon interactions, since they obviously cannot be neglected in the interpretation of the photoemission spectra.

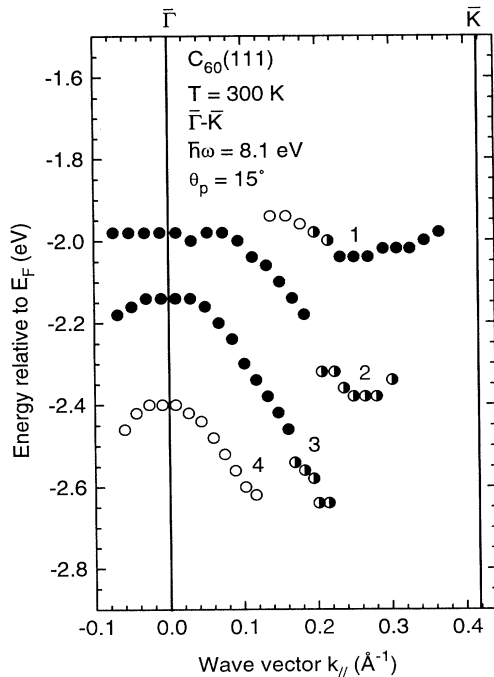


FIG. 3. Energy dispersion curves along the  $\bar{\Gamma}$ - $\bar{K}$  direction derived from the fitting procedure. The filled symbols represent the strongest peaks, the half-filled symbols less intense peaks, and the open symbols the least intense. The upper band at  $\bar{\Gamma}$  splits into two bands (1 and 2) with a maximum splitting of about 400 meV.

The observed dispersion in our photoemission spectra could also arise from relative variations of the matrix elements of the different bands, which would also change the photoemission line shape and shift the maxima with emission angle. At  $\hbar\omega = 8.1$  eV transitions are made to states just above the vacuum level which show a lot of structure (see, e.g., the inverse photoemission data by Jost *et al.*<sup>3</sup>) so final-state effects are highly plausible. Further experiments are in progress to separate the initial-state dispersion from the final-state effects. However, the shift of about 100 meV observed in  $\bar{\Gamma}$  with  $\hbar\omega = 29$  eV can be explained on basis of the spectra obtained with  $\hbar\omega = 8.1$  eV, which would not be the case if matrix elements played a significant role. As explained at the beginning, the small dispersion observed in the  $\bar{\Gamma}$ - $\bar{K}$  direction for  $\hbar\omega = 29$  eV is related to the poor  $k_{\parallel}$  resolution; each spectrum integrates information over 20% of the SBZ. For  $\hbar\omega = 8.1$  eV the analyzer covers only about 4% of the SBZ, so the band-structure information contained in the  $\hbar\omega = 29$  eV data can be simulated by adding up five successive EDC's recorded with  $\hbar\omega = 8.1$  eV in the  $\bar{\Gamma}$ - $\bar{K}$  direction. In Fig. 4 we show the result of the summation and compare it to the  $\hbar\omega = 29$  eV data. One can see that this operation eliminates the two components resolved at  $\hbar\omega = 8.1$  eV and considerably reduces the dependence of the line shape on emission angle. The dispersion of the maximum of the calculated photoemission spectrum is similar to that of the data measured at  $\hbar\omega = 29$  eV with a shift of about 100 meV at normal emission. This apparent shift is, therefore, real and results from averaging over the broad maximum around  $\bar{\Gamma}$  in the dispersion curve (see Fig. 3) which lowers the peak

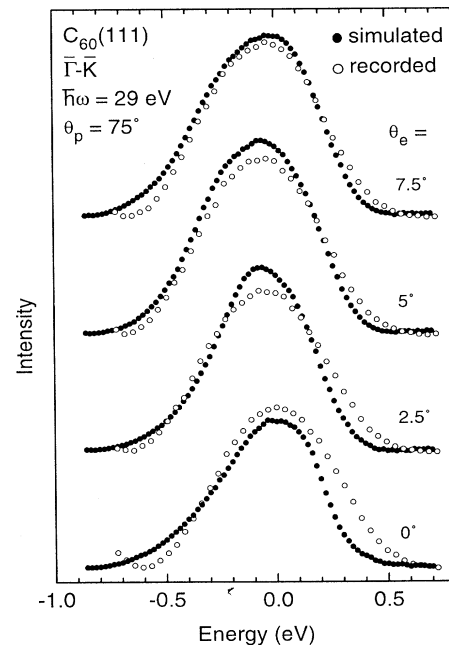


FIG. 4. Comparison between a set of simulated EDC's obtained by summing up five successive EDC's recorded at  $\hbar\omega = 8.1$  eV (filled symbols) and the EDC's recorded at  $\hbar\omega = 29$  eV (open symbols). The energy scale is referenced to the valence-band maximum at  $\bar{\Gamma}$ .

position at normal emission. Thus, we believe that the changes in the line shape with emission angle observed at  $\hbar\omega = 8.1$  eV result primarily from band dispersion and not from matrix element effects.

In conclusion, we have reported photoemission measurements on crystalline  $C_{60}(111)$  at low photon energy ( $\hbar\omega = 8.1$  eV), which present direct evidence of significant valence-band dispersion. Furthermore, we have shown that the photoemission line shape cannot be explained by phonon broadening alone, but band dispersion has also to be included. A detailed comparison between the experimental data presented here and more elabo-

rate theoretical calculations taking into account electron-phonon interaction should permit an improved determination of the band structure of  $C_{60}$  fullerite.

We thank G. Sawatzky for providing us with  $C_{60}$ . We acknowledge fruitful discussions with him and Ph. Lambin, S. G. Louie, A. A. Lucas, U. Karlsson, and J. H. Weaver. This work was supported by the European Community (Grant No. II91-15-EC), the Belgian national program of Interuniversity Research Projects, the Wallonia Region, and the BMFT under Project No. 05 5GUABI.

- 
- <sup>1</sup> S. Saito and A. Oshiyama, *Phys. Rev. Lett.* **66**, 2637 (1991).
- <sup>2</sup> J. H. Weaver, J. L. Martins, T. Komeda, Y. Chen, T. R. Ohno, G. H. Kroll, N. Troullier, R. E. Haufler, and R. E. Smalley, *Phys. Rev. Lett.* **66**, 1741 (1991).
- <sup>3</sup> M. B. Jost, N. Troullier, D. M. Poirier, J. L. Martins, J. H. Weaver, L. P. F. Chibante, and R. E. Smalley, *Phys. Rev. B* **44**, 1966 (1991).
- <sup>4</sup> B. Wästberg and A. Rosén, *Phys. Scr.* **44**, 276 (1991).
- <sup>5</sup> D. L. Lichtenberger, M. E. Jatcko, K. W. Nebesny, C. D. Ray, D. R. Huffman, and L. D. Lamb, in *Clusters and Cluster-Assembled Materials*, edited by R. S. Averback, J. Bernholc, and D. L. Nelson, MRS Symposia Proceedings No. 206 (Materials Research Society, Pittsburgh, 1991), p. 673; D. L. Lichtenberger, K. W. Nebesny, C. D. Ray, D. R. Huffman, and L. D. Lamb, *Chem. Phys. Lett.* **176**, 203 (1991).
- <sup>6</sup> N. Troullier and J. L. Martins, *Phys. Rev. B* **46**, 1754 (1992).
- <sup>7</sup> J. Wu, Z.-X. Shen, D. S. Dessau, R. Cao, D. S. Marshall, P. Pianetta, I. Lindau, X. Yang, J. Terry, D. M. King, B. O. Wells, D. Elloway, H. R. Wendt, C. A. Brown, H. Hunziker, and M. S. de Vries, *Physica C* **197**, 251 (1992).
- <sup>8</sup> J.-M. Themlin, S. Bouzidi, F. Coletti, J.-M. Debever, G. Gensterblum, L.-M. Yu, J.-J. Pireaux, P. A. Thiry, and R. Caudano, *Phys. Rev. B* **46**, 15 602 (1992).
- <sup>9</sup> G. Gensterblum, L.-M. Yu, J.-J. Pireaux, P. A. Thiry, R. Caudano, J.-M. Themlin, S. Bouzidi, F. Coletti, and J.-M. Debever, *Appl. Phys. A* **56**, 175 (1993).
- <sup>10</sup> P. A. Heiney, J. E. Fischer, A. R. McGhie, W. J. Romanow, A. M. Devenstein, J. P. McCauley, Jr., A. B. Smith III, and D. E. Cox, *Phys. Rev. Lett.* **66**, 2911 (1991).
- <sup>11</sup> Spectrum Square Associates, Inc.